

PROCEEDINGS OF SPIE

[SPIDigitalLibrary.org/conference-proceedings-of-spie](https://spiedigitallibrary.org/conference-proceedings-of-spie)

EUV low-n attenuated phase-shift mask on random logic via single patterning at pitch 36nm

Ling Ee Tan, Werner Gillijns, Jae Uk Lee, Dongbo Xu, Jeroen van de Kerkhove, et al.

Ling Ee Tan, Werner Gillijns, Jae Uk Lee, Dongbo Xu, Jeroen van de Kerkhove, Vicky Philipsen, Ryoung-Han Kim, "EUV low-n attenuated phase-shift mask on random logic via single patterning at pitch 36nm," Proc. SPIE 12051, Optical and EUV Nanolithography XXXV, 120510P (26 May 2022); doi: 10.1117/12.2614000

SPIE.

Event: SPIE Advanced Lithography + Patterning, 2022, San Jose, California, United States

EUV low-n attenuated phase-shift mask on random logic Via single patterning at pitch 36nm

Ling Ee Tan*, Werner Gillijns, Jae Uk Lee, Dongbo Xu, Jeroen Van de Kerckhove, Vicky Philipsen, Ryoung-han Kim
IMEC, Kapeldreef 75, B-3001 Leuven, Belgium

ABSTRACT

Imec N3 logic design rules define a minimum via pitch of 36nm for a double patterning process. Enabling this pitch is crucial in terms of process time and number of masks involved. One method for extending 0.33 NA EUV is using advanced mask materials. Studies have shown that a low-n attenuated phase-shift mask (PSM) can improve EUV imaging performance, reduce mask 3D effects and improve optical contrast compared to the reference Ta-based mask. [1-3]

In this paper, the impact of mask stack - Ta-based (binary or BIM) and low-n (PSM) - and mask tone - dark field (DF) vs. bright field (BF) - on a random logic Via layer will be evaluated. To pattern contact holes, we use negative tone development (NTD) metal-oxide resist process using the BF mask and positive tone development (PTD) chemically amplified resist process using the DF mask. Source mask optimization (SMO) was performed with and without sub-resolution assist feature (SRAF) as a resolution enhancement technology (RET). Optical proximity correction (OPC) was carried out on design clips using respective sources and mask rules at different mask tone. We show the optimum choice for this layer and present our recommendation based on current OPC simulations as well as some preliminary wafer data.

Keywords: Computational lithography, 36nm pitch contact hole, random logic Via, mask tone, low-n PSM mask, Bright Field, Dark Field, OPC

1. INTRODUCTION

Imec N3 logic design Vint (middle of line Via), which connects GATE/M0A and first metal layer, is gridded on Mint (middle of line metal) horizontally oriented at pitch 18nm CD 9nm and on Gate/M0A at pitch 42nm CD 18nm vertically oriented. Thus, giving us the design target of CDx 18nm by CDy 9nm. The device integration scheme is semi damascene SAC (self-aligned contact) in x direction, giving us the possibility to apply a reasonable litho bias. Our litho target Via design will be elongated at Pitch X 42nm CDx 26nm and Pitch Y 36nm CDy 18nm (Figure 1).

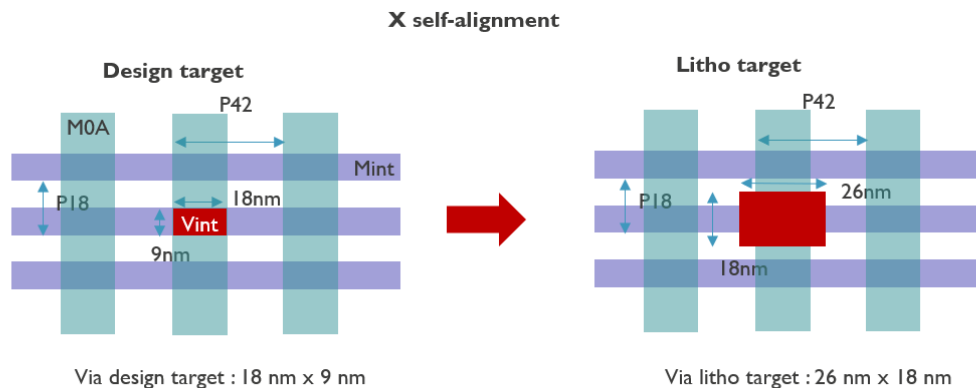


Figure 1. Imec Via design target and litho target

*ling.ee.tan@imec.be

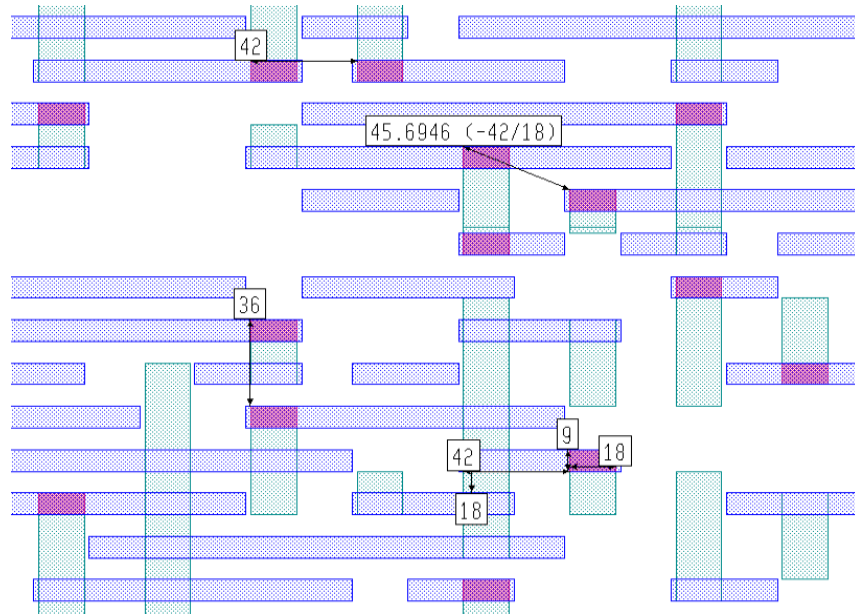


Figure 2. Ivec random logic Via design target on Mint and MOA grid

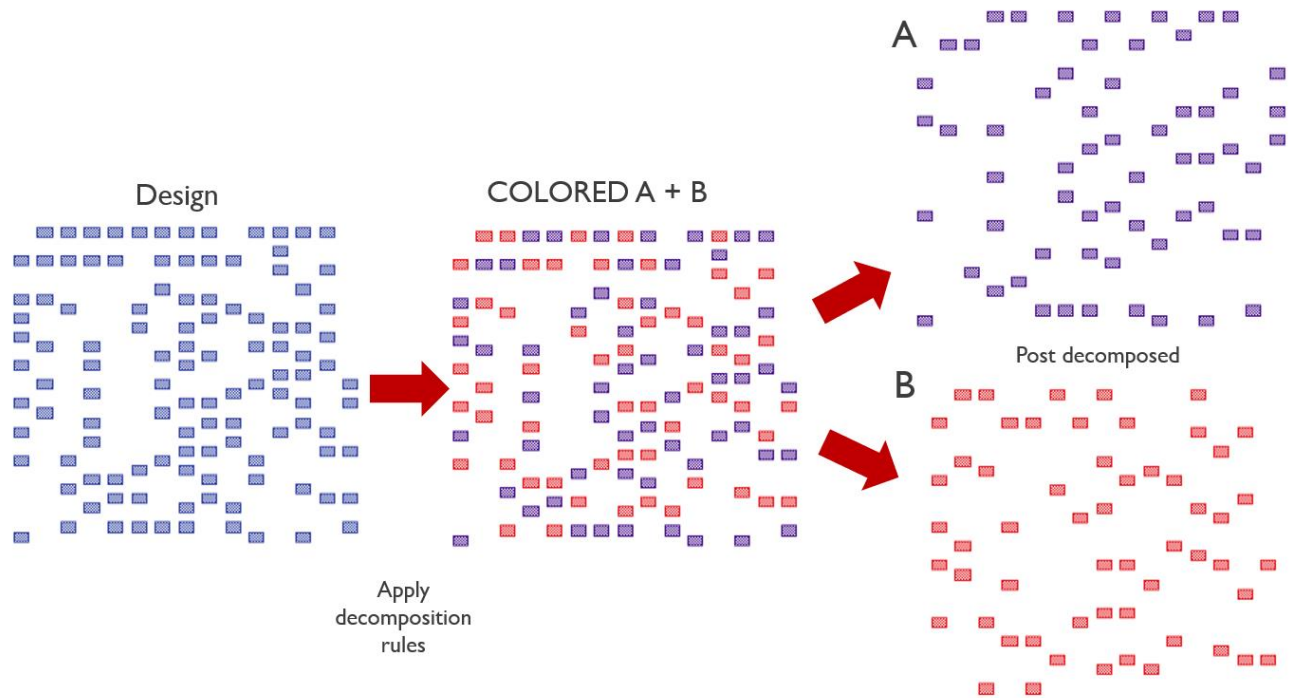


Figure 3. Ivec random logic Via from design to post decomposed (2 color scheme)

Figure 2 illustrates the random Via on Mint and MOA grid, we see here some of the most common configurations of doublet X (2 vias in X – side by side) at pitch X 42nm, doublet Y (2 vias in Y – top bottom skipping 1 Mint pitch) at pitch 36nm, and doublet diagonal at C2C (center-to-center) at 45.7nm (pitch X 42nm, pitch Y 18nm). Figure 3 illustrates imec random logic Via from design to post decomposition of 2 color masks, we try to keep an optimal and balanced density on both

masks. Enabling these pitches would be a gain to lower cost of manufacturing by considering double patterning with litho-etch-litho-etch (LELE) process instead of triple patterning LELELE process.

In this paper, a low-n mask (PSM) is being evaluated together with a Ta-based mask (BIM) as a reference. Studies have shown that PSM can improve EUV imaging performance since it could reduce mask 3D effects and improve optical contrast compared to BIM. [1-3] However, EUV PSM has bigger phase difference and higher transmission of up to 30% bringing concern on how such exposures would be affected by side-lobe printing. [7]

We obtained simulation results from the Tachyon ASML SMO tool for different mask types and tones as well as for sub-resolution assist feature on selected mask approaches. For these different options we compare process variation (PV) bands, normalized image log-slope (NILS), mask error enhancement factor (MEEF), and best focus shifts of the selected vias. We report on the experimental evaluation of our first iteration OPC result on wafer.

2. SIMULATION

Our simulation settings are as follows, the default EUV SMO template for NXE3400 is used, pupil efficiency is set to 100%, constant 2% flare level, and process window metric of $\pm 10\%$ delta dose and $\pm 40\text{nm}$ delta focus is being considered. The input clips will be described in each section.

We included two different mask absorbers - Ta-based mask (BIM) and low-n mask (PSM) - and two different mask tones, - bright field (BF) and dark field (DF). Simulations are aerial image with a 3nm aerial image blur to mimic the resist process. SMO-MO (Mask Optimization) flow is used to evaluate different splits to allow model to reach optimal threshold, best focus, and mask correction. [8] MRC (Mask Rule Check) is applied to the input clips according to mask shop specifications on both mask tones respectively. In the next Section, we will motivate our choices for our test case based on simulations.

2.1 Array test pattern on fixed source versus source mask optimization

Array test patterns of CD 20nm square contact holes at pitch 40nm, 60nm and 100nm are evaluated by Mask Optimization (MO) using a fixed source (Quasar) and compared to SMO results. Splits of mask type and mask tone will be discussed. The following will be our naming convention BBF (Binary Bright Field mask), BDF (Binary Dark Field mask), PBF (PSM Bright Field mask) and PDF (PSM Dark Field mask).

Pitch [nm@1x] = 40,

60

100

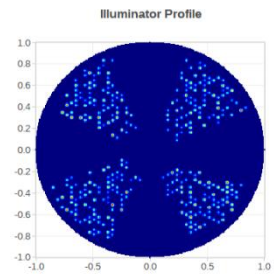
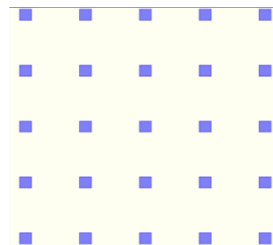
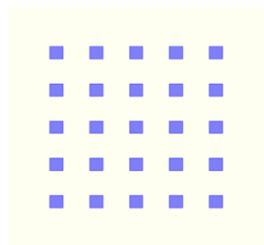


Figure 4. Array of square contact holes at pitch 40, 60, 100nm and Quasar source on far right.



Figure 5. Histogram plot of NILS at best focus and MEEF at CD20 X cutlines of pitch 40, 60 and 100nm. (Orange - reference BDF, blue BBF, grey PBF, yellow PDF)



Figure 6. Histogram plot of PV Band (process variation band), best focus shift at CD20 X cutlines of pitch 40, 60 and 100nm. (Orange - reference BDF, blue BBF, grey PBF, yellow PDF)

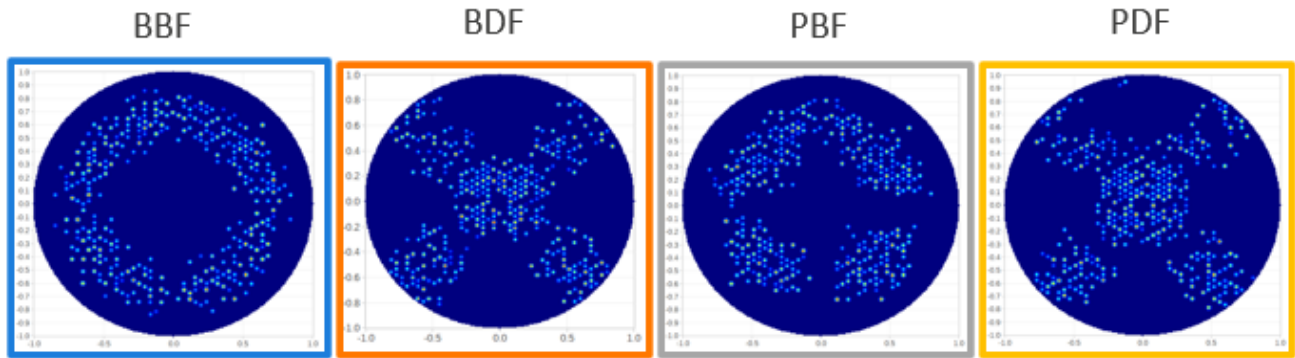


Figure 7. SMO optimized sources on array CD20 at pitch 40nm, 60nm and 100nm (Orange - reference BDF, blue BBF, grey PBF, yellow PDF)

The top row of Figure 5 shows NILS improvement at pitch 40nm CD 20nm for PSM over BIM for both tonalities BF and DF for the MO fixed Quasar source. At pitch 60nm and 100nm, PBF has higher NILS compared to BBF, while PDF does not gain NILS compared to BDF. MEEF improves for all pitch using PSM over BIM, and this for both tonalities.

The top row of Figure 6, the MO fixed Quasar source result shows the PV bands for the different mask types. There is an overall improvement for PBF over BBF, but PDF only improves the smallest pitch 40nm over BDF. Best focus shifts, plotted in Figure 6, are largest for PDF, and may restrict the overlapping process window (OPW).

The bottom row in Figure 5 and 6 represents the SMO results on the four splits and shows improved performance over the Quasar source on three metrics: NILS, PV Band and best focus shift. Average MEEF improves for BBF, but there are no significant MEEF improvement for BDF, PDF and PBF compared to the quasar source (MO).

Comparing within the SMO group, BBF shows good NILS, MEEF and PV Band, while best focus shift is reasonable. The SMO optimization on BBF enhanced NILS on all features, the order of NILS improvement has changed especially on DF mask. With this, we conclude that SMO is preferred to enhance image contrast and to have better CD control.

2.2 Random logic Via SMO

On random logic Via, we use target design clips as shown in Figure 8 for SMO optimization. We include all possible Via on Mint and Gate/M0A grid configurations at pitch x 42nm pitch y 36nm CDx 26nm CDy 18nm, consisting of square array, staggered array, doublets (DD, DX, DY), isolated, triplets (T3A, T3B, T3C, T3D, T3E, T3F, T3G), cluster of four vias (C4A, C4B), cluster of five vias (C5A), rows in X (RowX, ZZx), rows in Y (RowY, ZZY) and diagonal rows (Diagonal, Diagonal2).

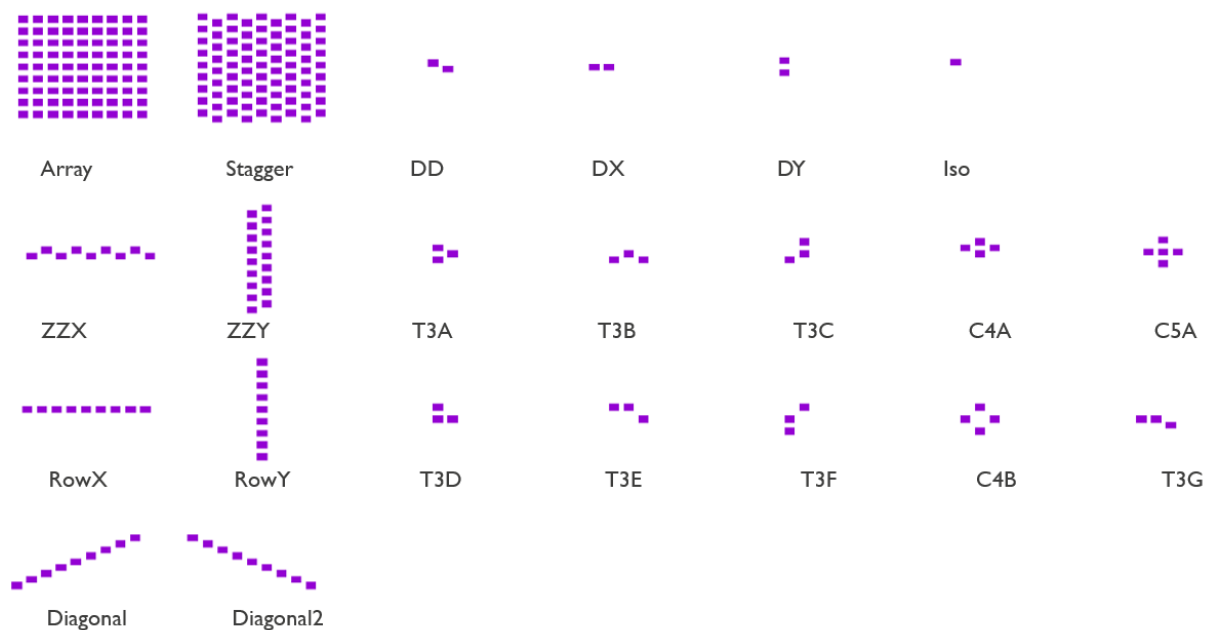


Figure 8. SMO optimization input clips

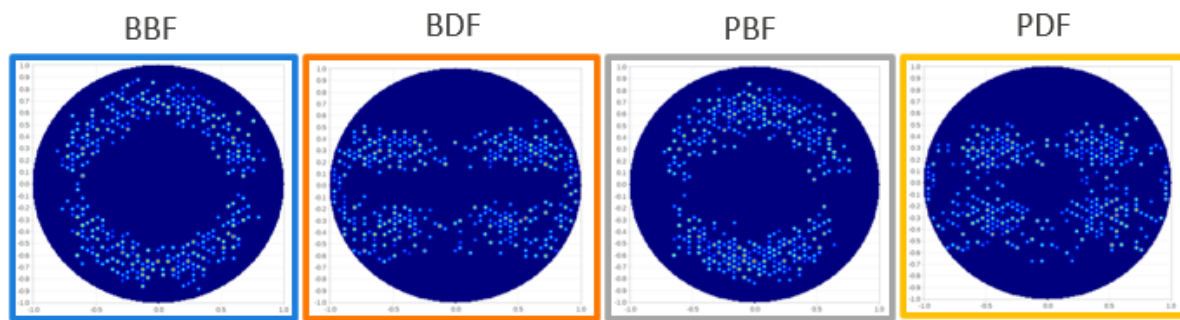


Figure 9. SMO optimized sources on random logic clips (Orange - reference BDF, blue BBF, grey PBF, yellow PDF)



Figure 10. Histogram plots of NILS at best focus, MEEF, PV Band (process variation band), Best focus shift at pitch x 42nm pitch y 36nm designs: array, iso, doublet X (DX), doublet Y (DY), and doublet diagonal (DD) (Orange - reference BDF, blue BBF, grey PBF, yellow PDF)

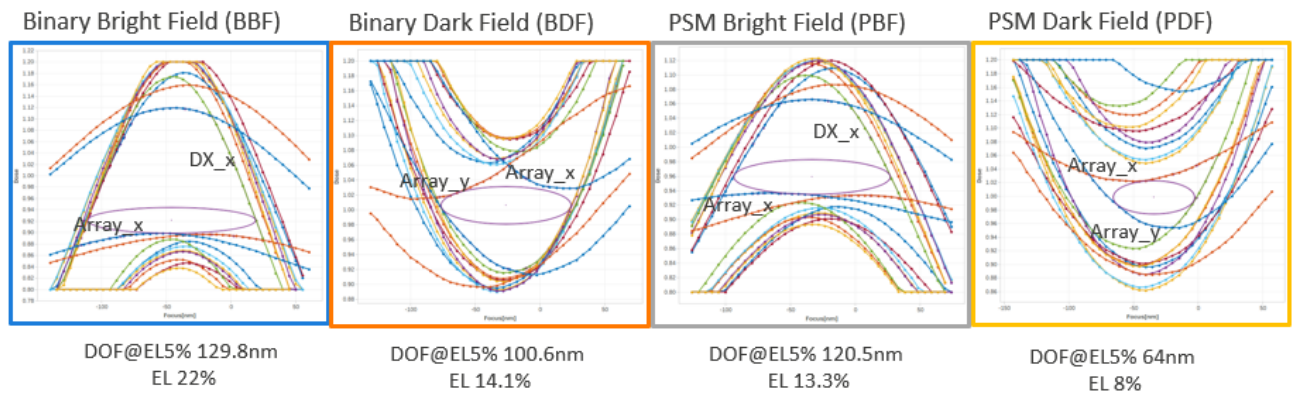


Figure 11. Overlapping Process Window (OPW), Depth-of-Focus (DOF) and Exposure Latitude (EL) at pitch x 42nm pitch y 36nm designs: array, iso, doublet X (DX), doublet Y (DY), and doublet diagonal (DD) (Orange - reference BDF, blue BBF, grey PBF, yellow PDF). Process windows calculated for CD tolerance of 15% and PDF CDx was relaxed to 24nm on the array.

We selected array, doublets diagonal (DD), doublets X (DX), doublets Y (DY) and isolated clip as our represent clip on random logic design to further understand the imaging performance. Figure 10 compares the SMO on random logic via clips on the four mask types for the four metrics, NILS, MEEF, PV band and best focus. On the DF tone design, the PSM

improves all four metrics compared to BIM. For the BIM, the BF tone design are better for all four parameters NILS, MEEF, PV band and best focus shift with respect to the DF tone. Lastly, comparing BBF to PBF, there is no advantage on NILS, MEEF, PV band and BF shift.

Figure 11 presents the overlapping process window (OPW) for the four mask types. It is observed that the Depth-of-Focus (DOF) of BDF to PDF is reduced from 100.6nm to 64nm with an exposure latitude (EL) drop from 14.1% to 8%. The array pattern is the PW limiter in both cases. For the PDF, the best focus shift of array-x away from the optimal best focus of the other designs. For the BBF an increase of overlapping PW is seen with respect to BDF (cf. Figure 11); DOF grows to 129.5nm and EL to 22%. Comparing the overlapping PW of BBF to PBF shows a DOF reduction from 129.8nm to 120.5nm and EL reduction from 22% to 13.3%. We can see that the BF mask - regardless BIM or PSM - shows larger DOF and EL compared to both DF masks. The PW limiters are the same for both BIM and PSM mask: for the BF tone the designs Dx_x and Array_x, and for the DF tone the designs Array_x and Array_y. The OPC convergence on this dense array suffers most from the MRC space limitation on the CD, leading to best focus shifts which lowers the overlapping DOF and therefore limiting the OPW.

Figure 12 shows the OPC correction of reference BDF and PDF. PDF OPC correction has reached the MRC space limit of 11.3nm with the contours printing at 24nm. The result raises the question of whether we could increase the dose and allow the mask correction to be smaller. A series of OPC corrections was performed on different model thresholds to find a better threshold to size. As shown in Table 1, applying different model thresholds reduces the edge placement error (EP) of DD from 3nm to 1.3nm, whereas the EP on DX can be reduced from 2.6nm to 1.7nm. However, side lobe printing is seen when the threshold of the model is below 0.055, which corresponds to high exposure dose. We tried to mitigate the side lobe printing by optimizing the mask CD without success. Side lobe printing is more severe on PSM DF mask because the mask absorber reflectivity for low-n absorber (~13%) is elevated compared to the TaBN (2%) absorber. This dose evaluation shows that DF PSM for logic via must balance the OPC limited by MRC and sidelobe printability.

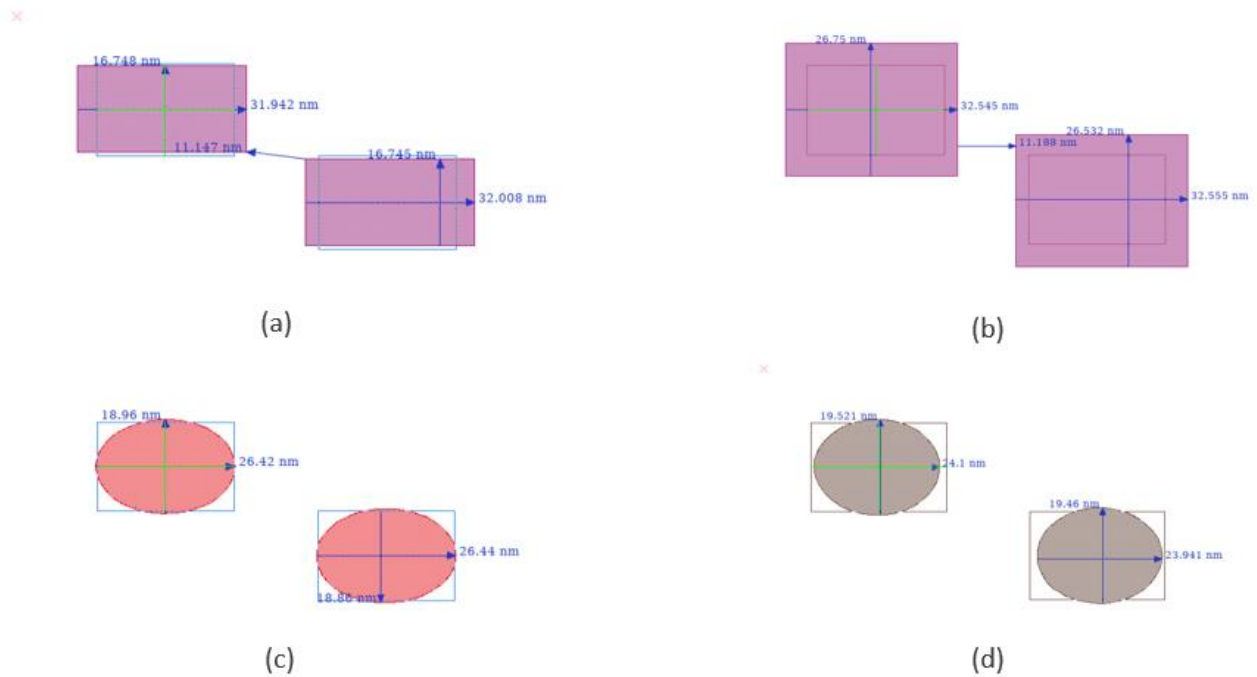


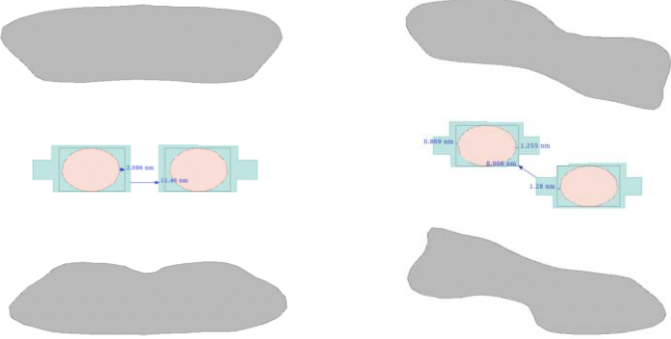
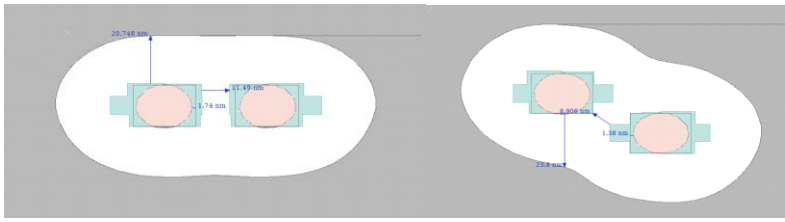


Figure 12. OPC correction example on reference BDF versus PDF mask. (a) BDF OPC correction (b) PDF OPC correction (c) BDF OPC contour (d) PDF OPC contour.

Table 1. OPC correction and resulting contours of the doublets DD and DX on the PDF model at different model thresholds (first column). Third column lists the EP values and the sidelobe (SL) occurrence.

| Model threshold | OPC correction | Remarks |
|-----------------|---|---|
| 0.0605 |  | DX EP 2.6nm DD EP 3.0nm No side lobe (SL) printing |
| 0.055 |  | DX EP 2.4nm DD EP 2.8nm No SL printing |
| 0.0505 |  | DX EP 2.1nm DD EP 1.3nm SL printing ~28nm from main feature |
| 0.045 |  | DX EP 1.7nm DD EP 1.3nm SL printing ~20nm from main feature |

2.3 SRAF insertion

In this section, we elaborate on possibility of SRAF insertion in our test case. We evaluate BF and DF BIM and PSM for the input clips of Figure 8. We compare each split of mask type and mask tone on its own with and without SRAF. We notice that three metrics; NILS, PV band and best focus shift improves with SRAF insertion for PSM DF and BF as well as for BIM DF. On the other hand, SRAF insertion for the BBF mask has no significant improvement on NILS, PV band and best focus shift. MEEF becomes worst with SRAF insertion except for BDF, as can be seen in Figure 13 and Figure 10. SRAF insertion reduces the best focus shift across different features compared to no SRAF insertion.

Inserting SRAFs can help enlarge OPW and EL for most cases except BIM BF (cf. Figure 14 and Figure 11). BDF compared to BDF with SRAF, DOF at 5%EL is enlarged from 100.6nm to 143nm with EL increase from 14.1% to 17.5%, PBF to PBF with SRAF, we see DOF increased from 120.5nm to 140.2nm with EL increase from 13.3% to 14.5%. A significant OPW improvement of PDF to PDF with SRAF where DOF increased from 64nm to 125.3nm with EL increase from 8% to 13.6%. The comparison of the OPW for BBF to BBF_wAF shows that the exposure latitude (EL) is reduced from 22% on BBF to 17.3% on BBF_wAF and that the DOF at 5%EL is decreased from 129.8nm to 117.1nm.

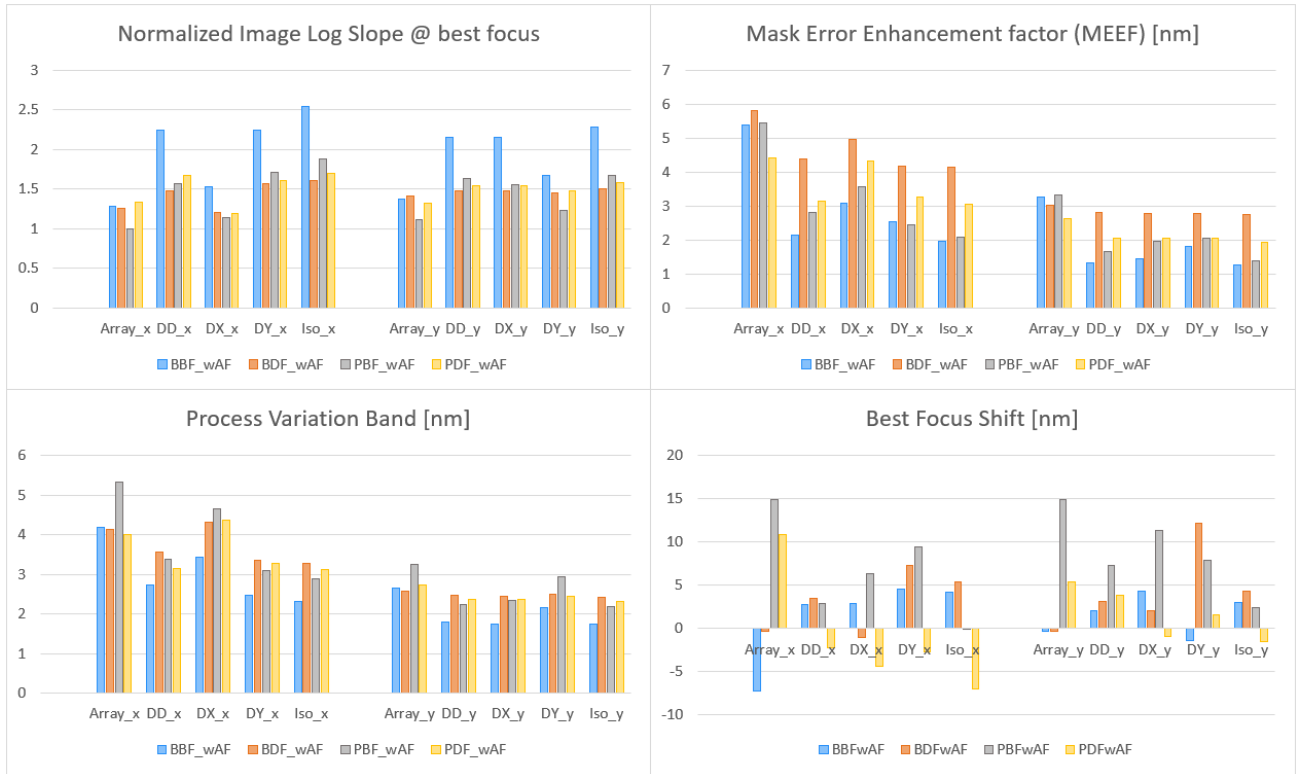


Figure 13. Histogram plot of NILS at best focus, MEEF, PV Band (process variation band), best focus shift at selected designs: array, iso, doublet X (DX), doublet Y (DY), and doublet diagonal (DD) (light blue BBF_wAF, light orange BDF_wAF, light grey PBF_wAF, light yellow PDF_wAF (with assist-feature))

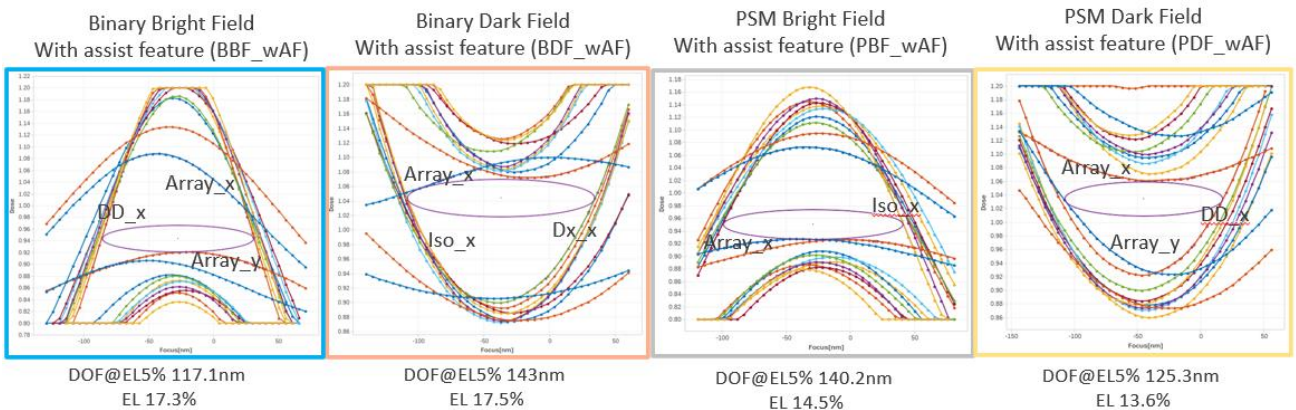


Figure 14. Overlapping Process Window (OPW) and Exposure Latitude (EL) at selected designs: array, iso, doublet X (DX), doublet Y (DY), and doublet diagonal (DD) (light blue BBF_wAF, light orange BDF_wAF, light grey PBF_wAF, light yellow PDF_wAF (with assist-feature)). Plots at CD tolerance of 15%.

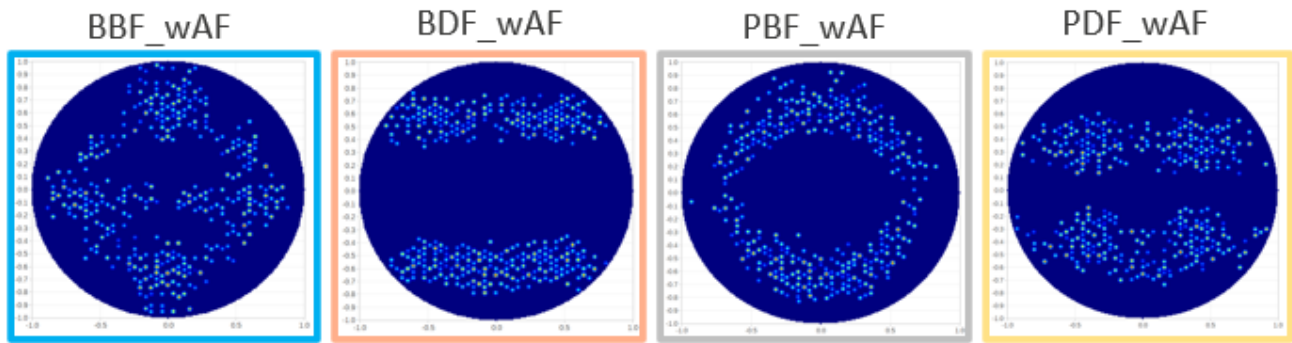


Figure 15. SMO optimized sources on random logic clips (light blue BBF_wAF, light orange BDF_wAF, light grey PBF_wAF, light yellow PDF_wAF)

Table 2. Summary table for metrics; NILS, MEEF, PV Band, Best focus shift, DOF@5% and EL on Binary and PSM mask type, bright field and dark field mask tone, without and with SRAF insertion for random logic generic features.

| | | Binary | | PSM (low-n) | |
|---------|-------------------------------|--------------|------------|--------------|------------|
| | | Bright Field | Dark Field | Bright Field | Dark Field |
| No SRAF | NILS (min) | 1.45 | 0.98 | 0.92 | 1.00 |
| | MEEF (max) | 4.04 | 8.95 | 4.61 | 4.22 |
| | PV Band [nm] (max) | 4.3 | 5.3 | 5.8 | 4.2 |
| | Best focus shift [nm] (range) | 10.3 | 39.5 | 20.2 | 25.3 |
| | DOF @ 5%EL | 129.8 | 100.6 | 120.5 | 64.0 |
| | EL (max) | 22 | 14.1 | 13.3 | 8.0 |
| SRAF | NILS (min) | 1.29 | 1.20 | 1.00 | 1.19 |
| | MEEF (max) | 5.38 | 5.82 | 5.45 | 4.41 |
| | PV Band [nm] (max) | 4.2 | 4.3 | 5.3 | 4.4 |
| | Best focus shift [nm] (range) | 11.9 | 13.3 | 15.0 | 17.8 |
| | DOF @ 5%EL | 117.1 | 143.0 | 140.2 | 125.3 |
| | EL (max) | 17.3 | 17.5 | 14.5 | 13.6 |

2.4 Random logic clip (Design)

We want to further understand the eight mask splits on imec N3 random logic design, thus we performed mask optimization on single color post decomposed random logic Via (cf. Figure 16.), which is 1.5um by 1.5um with a total of 295 vias and 590 cutlines in x and y. We extract simulation results from each cutline on the simulation metrics: NILS, MEEF, PV band, best focus shift, DOF and EL.

We compare each split of mask type and mask tone on its own with and without SRAF. Figure 17 shows that SRAF insertion can improve NILS and PV band within each group splits. However, MEEF becomes worst with SRAF insertion except for BDF group. Figure 18 shows the overlapping process window for the splits, we notice that SRAF insertion on Ta-based mask does not bring much benefit on both bright field and dark field. For PSM mask, on the contrary, with SRAF insertion the overlapping process window can be widened, and most significant improvement is on PDF group: with SRAF insertion (PDF_wAF), the DOF at 5%EL is 82.8nm and max. EL is 8.7% from no process window on PDF without SRAF. We notice that the BF mask regardless BIM or PSM shows larger DOF and EL compared to DF mask. For the studied iN3

random logic via clips the SMO for BBF without SRAF outperforms the other mask types including SRAF. This is a beneficial result, since many factors such as SRAF size, SRAF distance to main and SRAF printability (sensitivity to dose or focus change) could make SRAF insertion a big challenge to implement.

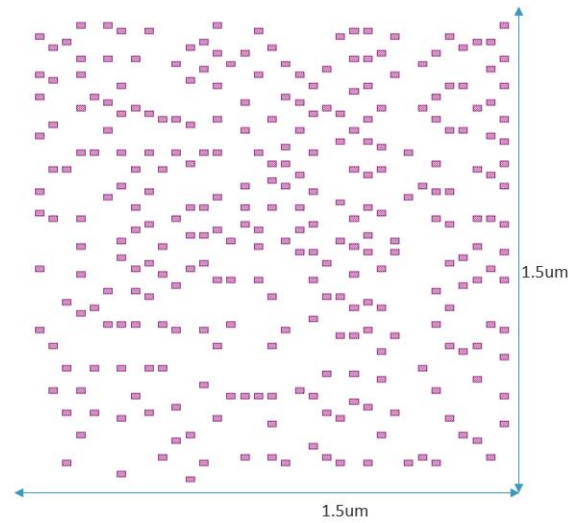


Figure 16. MO input clips on single color decomposed random logic via design, 1.5um x1.5um, 295 vias, 590 cutlines (x/y)

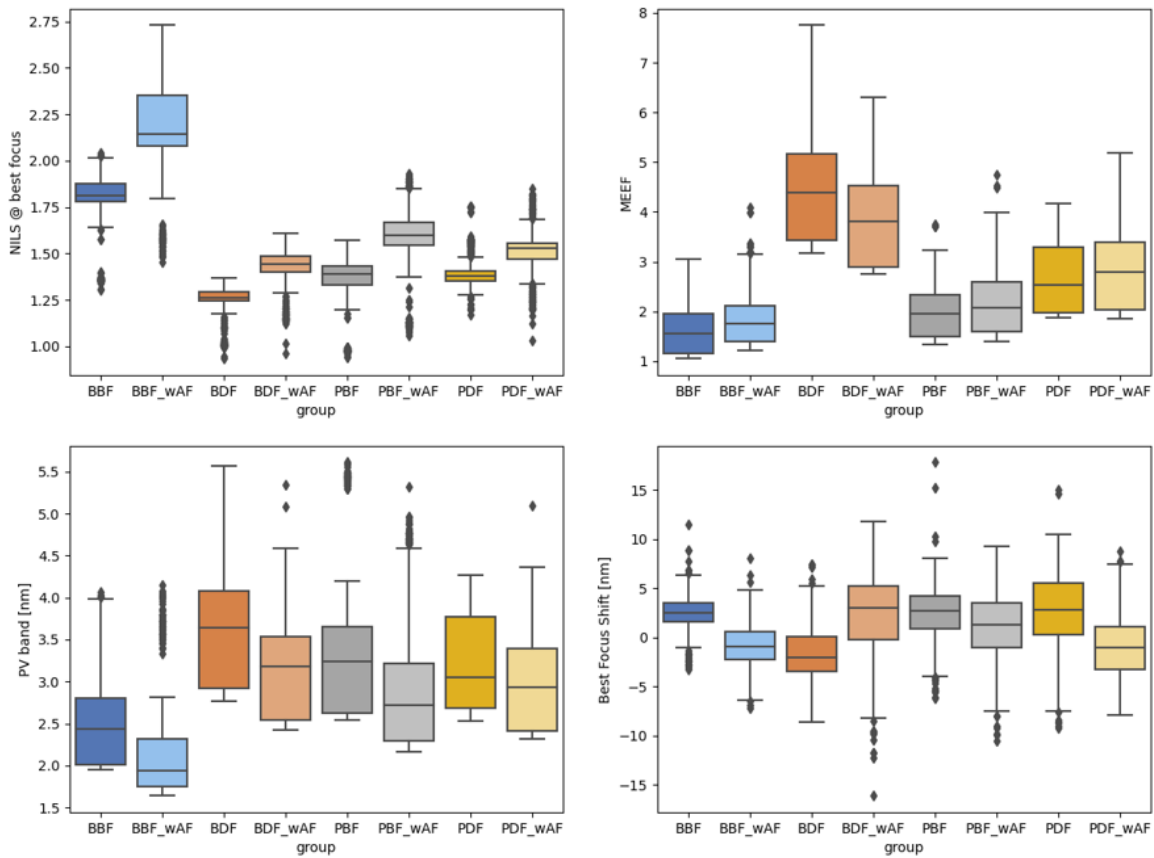


Figure 17. Box plot of Nils at best focus, MEEF, PV Band (process variation band), best focus shift on random logic via design (blue BBF, light blue BBF_wAF, orange BDF, light orange BDF_wAF, grey PBF, light grey PBF_wAF, yellow PDF, light yellow PDF_wAF (with assist-feature))

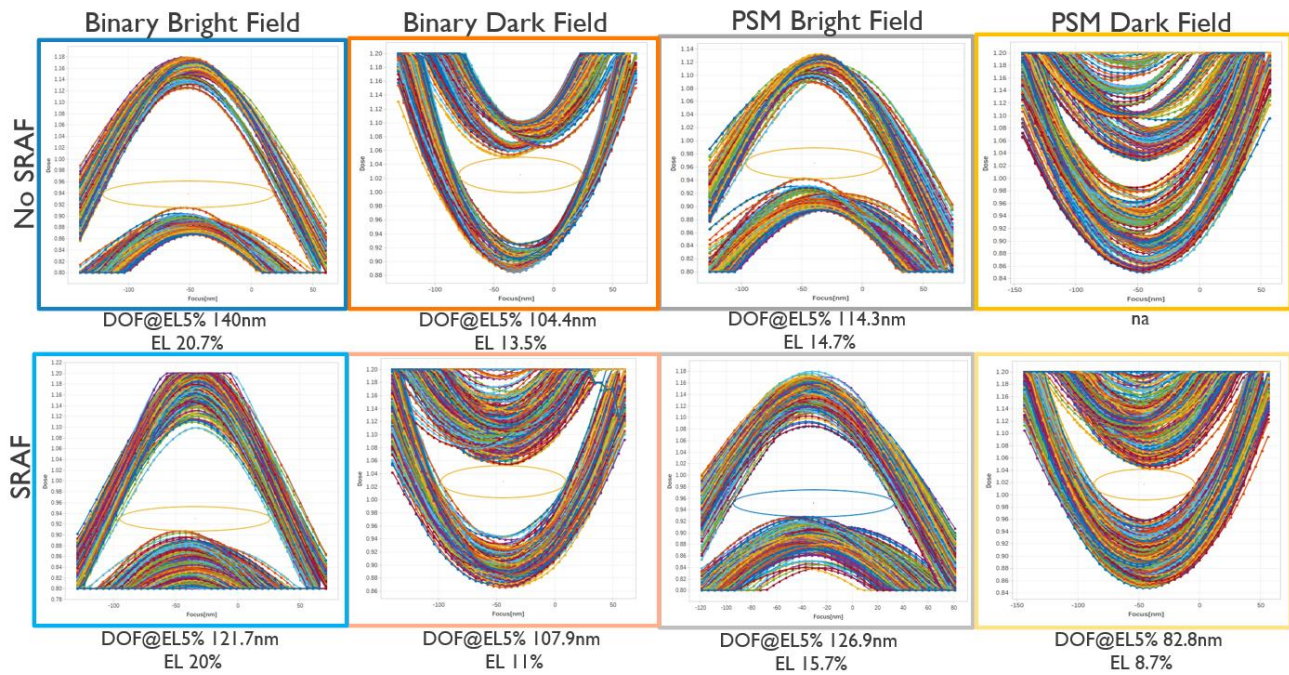


Figure 18. Overlapping Process Window (OPW) and Exposure Latitude (EL) from random logic via clip: Top row without SRAF and bottom row with SRAF, Left to right column; from binary bright field, binary dark field, psm bright field, psm dark field. Plots at CD tolerance of 15%.

Table 3. Summary table for NILS, MEEF, PV Band, Best focus shift, DOF@5% and EL on Binary and PSM mask type, bright field, and dark field mask tones, without and with SRAF insertion for random logic clips.

| | | Binary | | PSM (low-n) | |
|---------|-------------------------------|--------------|------------|--------------|------------|
| | | Bright Field | Dark Field | Bright Field | Dark Field |
| No SRAF | NILS (min) | 1.3 | 0.93 | 0.94 | 1.17 |
| | MEEF (max) | 3.06 | 7.75 | 3.74 | 4.16 |
| | PV Band [nm] (max) | 4.1 | 5.6 | 5.6 | 4.3 |
| | Best focus shift [nm] (range) | 14.8 | 16.1 | 24.0 | 24.2 |
| | DOF @ 5%EL | 140.0 | 104.4 | 114.3 | NA |
| | EL (max) | 20.7 | 13.5 | 14.7 | NA |
| SRAF | NILS (min) | 1.45 | 0.96 | 1.06 | 1.03 |
| | MEEF (max) | 4.08 | 6.31 | 4.74 | 5.19 |
| | PV Band [nm] (max) | 4.2 | 5.3 | 5.3 | 5.1 |
| | Best focus shift [nm] (range) | 15.3 | 27.9 | 19.8 | 16.7 |
| | DOF @ 5%EL | 121.7 | 107.9 | 126.9 | 82.8 |
| | EL (max) | 20 | 11.0 | 15.7 | 8.7 |

3. EXPERIMENTAL

3.1 Mask quality Dark Field versus Bright Field

The mask process for DF EUV masks was prioritized over BF to support the initial via layers targeted for EUV. Additionally, the DF mask designs limit the printing risk of multilayer blank defects. Figure 19 shows mask CDSEM images of PSM (low-n) dark field and bright field masks with design litho target of CDx 26nm and CDy 18nm. The bright field mask has larger CD errors relative to the design intent. Both masks were fabricated with the positive tone resist that is most appropriate for DF designs. In addition, exposed multilayer feature (DF CD) optimization was given more weight than absorber features (BF CD). Based on the current bright field mask errors relative to design target, we do not further discuss wafer results obtained from the BF PSM mask in this paper. Prioritization of the absorber mask features is required to bring bright field EUV mask quality to be on par with EUV DF mask quality for Via design. However, the BF pillar resolution is likely to remain worse than DF via resolution of inherent adhesion challenges.

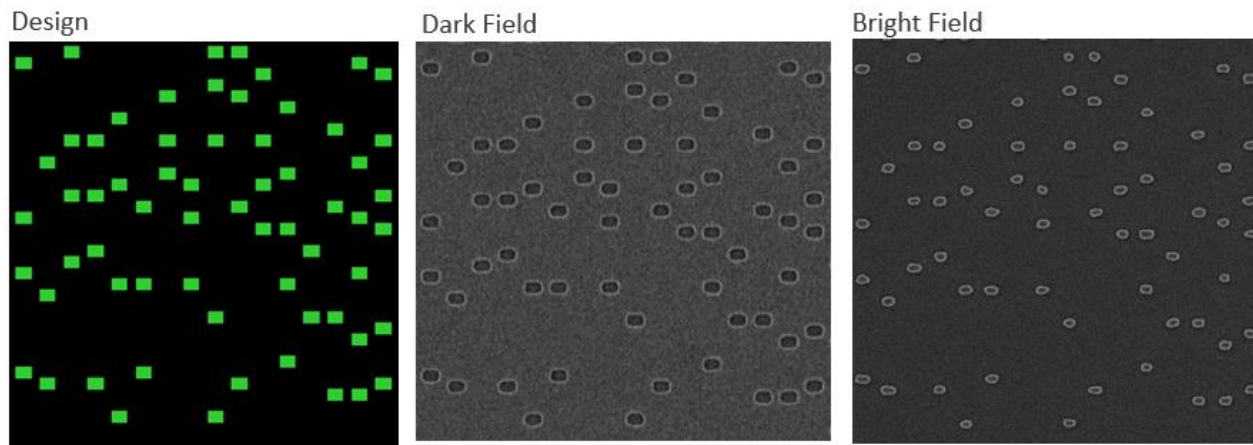


Figure 19. Mask design intent (left) vs. Mask CDSEM image on low-n dark field mask (middle) and bright field mask (left)

3.2 Dark Field wafer data

Wafer exposures were performed on the ASML 0.33NA NXE3400 EUV scanner at IMEC using development masks PSM DF and BIM DF. To pattern contact holes, we use positive tone development (PTD) chemically amplified resist process using the DF mask. Wafer results were analyzed from CDSEM (critical dimension scanning electron microscope) images (Hitachi) using IMEC's internally built tool ARCADI and Fractilia's MetroLER software.

In this section we will focus on the wafer evaluation of the via designs pitch x 42nm pitch y 36nm CDx 26nm CDy 18nm: array, iso, DD, DX and DY (see Figure 8) printed with dark field mask only. The target via designs went through first iteration of OPC with optical model respectively. Figure 20 shows the measured dose sensitivity across features in X and Y, PSM has lower dose sensitivity compared to BIM. Y cutlines show better dose sensitivity compared to X cutlines on both mask types. The overall trend correlates with the simulated NILS where the reverse trend is noticed on Array_y and DY_y. Optimal exposure dose is 49mJ/cm² with the PSM compared to 124mJ/cm² for the BIM, which is a 60% dose reduction using PSM mask (see Figure 21).

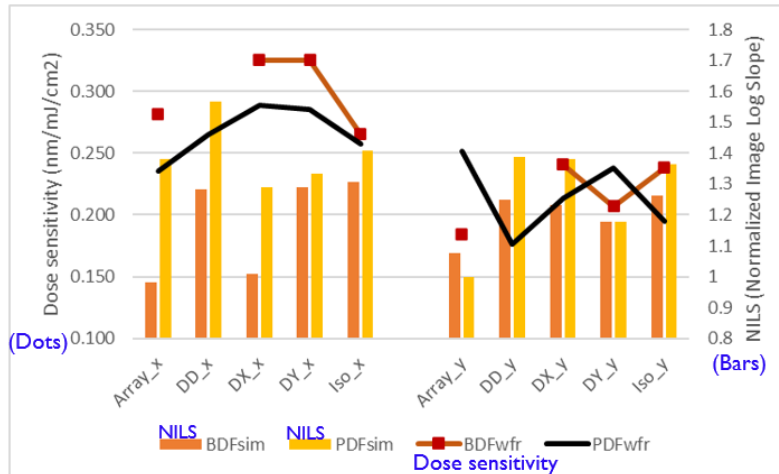


Figure 20. Simulated NLS (bars) and wafer Dose sensitivity (dots) across features in X and Y.

Figure 21 shows wafer SEM images in Focus Exposure matrix (FEM) for the doublet X (DX) on BIM DF mask (left) and PSM DF mask (right). Best focus and best dose are highlighted in red box, cyan box represents target CD within specification of 10% and lastly defect die in red. Defects from side lobe printing is more severe on higher dose starting from $>52\text{mJ}/\text{cm}^2$ leaving a small window for defect free process window across defocus. Side lobe printing is more sensitive to dose change than focus change. This is part of the challenge that was seen on PSM mask as compared to BIM mask.

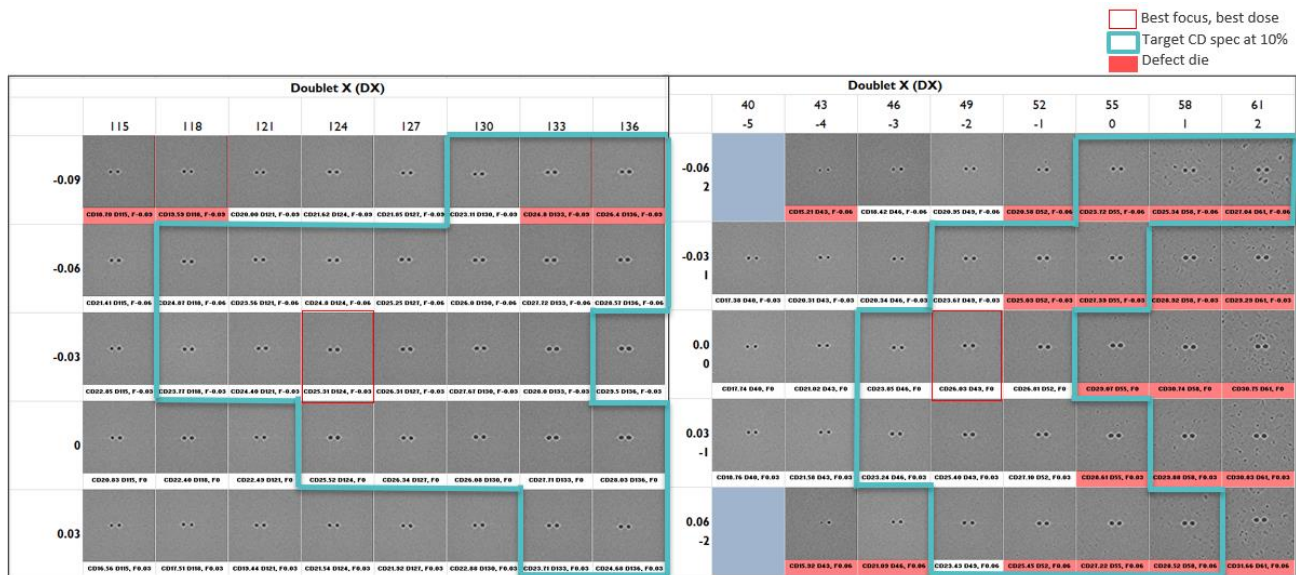


Figure 21. Focus Exposure Matrix (FEM) on Doublet X (DX) feature on BIM DF (left) and PSM DF (right). SL (Side Lobe) printing has become more severe as dose increases causing smaller defect free PW.

3.3 Random logic on PSM DF OPC solution

As we discussed in Section 2.2, we have noticed that MRC space at 11.3nm does not allow OPC to converge to target. To resolve this, we try two additional approaches, namely merged Via ^[4,5,6] and corner cut Via ^[6]. Merged Via approach is challenging as we need to ensure that the bridge polygon size complies to 10nm MRC minimum feature rule while simulation needs to show a defect free condition. As for corner cut via approach, a 5nm corner cut is performed when there

is a polygon corner opposing with a narrow space, targeting mainly diagonal doublet or triplet at narrow pitch Y 18nm or 36nm (refer OPC correction on Figure 22 left). A smaller OPC segment length is implemented on corner cut Via split. Figure 22 left shows the final OPC correction on random logic Via with the approach that we listed in addition to standard OPC (a) and OPC with SRAF (b). On the middle of Figure 22 a CDSEM image (819nm x 819nm) on wafer at best energy and best focus is exemplified. At the right of Figure 22 are histogram distribution plots of CDx and CDy for all Vias in the CDSEM images 819nm x 819nm. The optimal dose for standard OPC, merged vias and corner cut Via is at 49mJ/cm² since we apply the same model. As for OPC with SRAF insertion, we applied the respective model, thus the optimal dose is at 52mJ/cm².

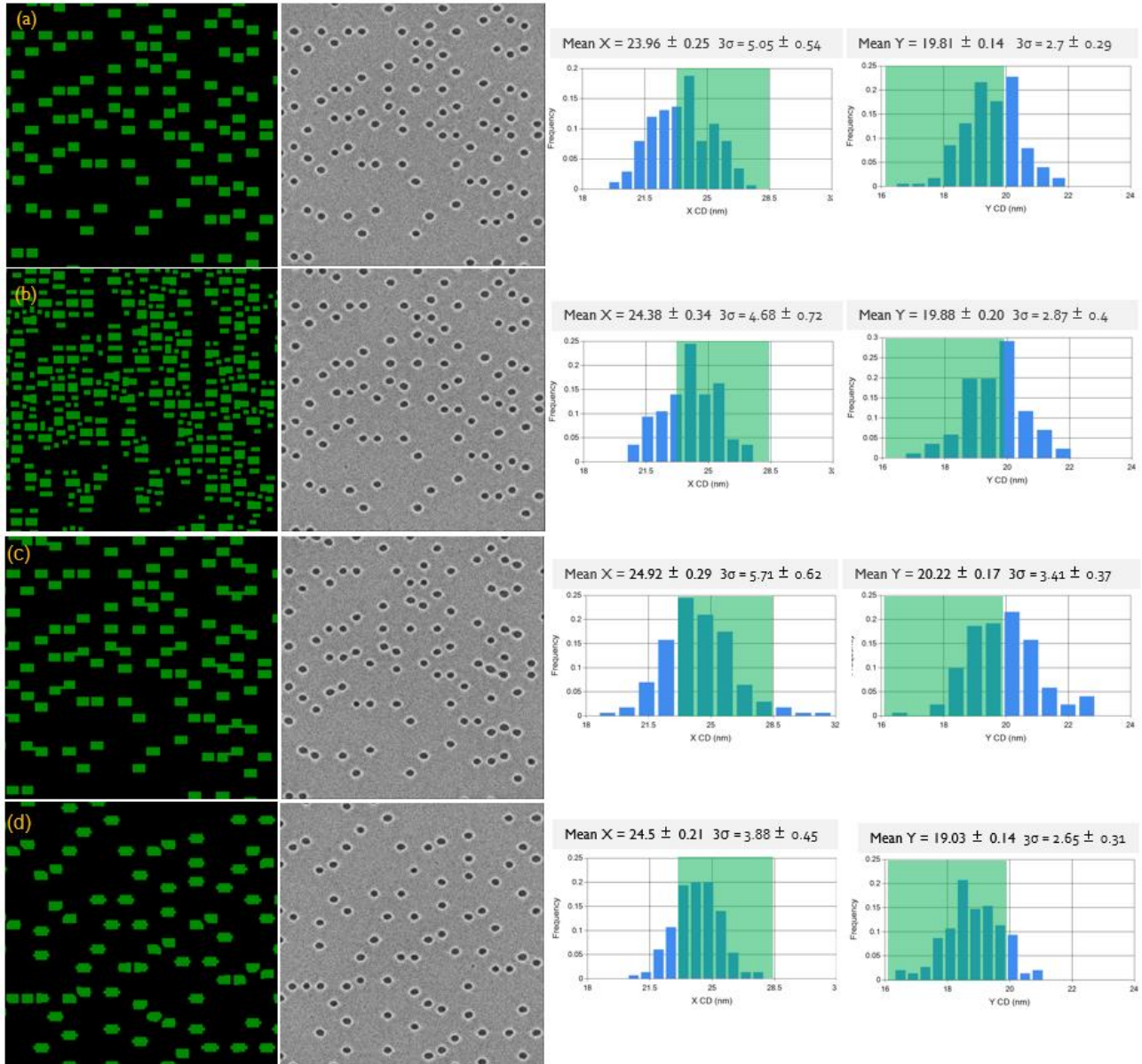


Figure 22. OPC corrections on PSM DF, CDSEM images at wafer optimal dose and focus and histogram plot of CDx and CDy. The target CD at ±10% spec is indicated by transparent green window. (a) standard OPC, (b) OPC with SRAF insertion (c) merged vias on diagonal adjacent vias, (d) corner cut via with smaller segments.

The Merged Via (c) approach was performed only on diagonal vias, CDx and CDy are enlarged to 25.5nm and 21nm respectively. This method is difficult to control as some of the vias are nearly bridging. The effect becomes more severe when there is a dose or focus change, thus limiting the overlapping PW. This approach can only target diagonal design, thus, to enhance full design CDx with this method is not possible.

The corner cut with small OPC run segment length (d) approach gives the best performance to target for CDx 26nm and CDy 18nm, which is 24.5nm and 19.0nm. Using smaller OPC run segment lengths creates more opportunities for OPC to converge to target while respecting the MRC rules. Small segment y can be seen in most of the Vias, allowing the middle segment to move out creating more elongated Vias compared to the other three splits.

For better comparison, Table 4 shows statistic comparison results from CDSEM images per OPC condition. The iso design converged best, followed by DY. DD can be improved using corner cut or merged via with a risk of bridging, leaving DX design as the most difficult to resolve.

Table 4 Statistics of overall vias measured per image, breakdown of DD, DX, DY, Iso vias according to OPC corrections (a) standard OPC, (b) OPC with SRAF insertion (c) merged vias on diagonal adjacent vias, (c) corner cut via with smaller segments.

| Statistics (nm) | Standard OPC | OPC with SRAF | Merged Vias | Corner Cut Vias |
|-------------------------|---|---|--|---|
| All Vias in CDx and CDy | Mean X = 23.96 ± 0.25 3σ = 5.05 ± 0.54 Mean Y = 19.81 ± 0.14 3σ = 2.7 ± 0.29 | Mean X = 24.37 ± 0.34 3σ = 4.68 ± 0.72 Mean Y = 19.88 ± 0.20 3σ = 2.87 ± 0.4 | Mean X = 24.88 ± 0.29 3σ = 5.72 ± 0.62 Mean Y = 20.19 ± 0.17 3σ = 3.40 ± 0.37 | Mean X = 24.5 ± 0.21 3σ = 3.88 ± 0.45 Mean Y = 19.03 ± 0.14 3σ = 2.65 ± 0.31 |
| Diagonal Doublet (DD) | Mean X = 23.1 ± 3.4 Mean Y = 19.6 ± 2.8 | Mean X = 23.5 ± 1.4 Mean Y = 19.9 ± 1.0 | Mean X = 25.5 ± 1.7 Mean Y = 21 ± 1.1 | Mean X = 25.0 ± 0.4 Mean Y = 19.2 ± 0.2 |
| Doublet X (DX) | Mean X = 23.0 ± 2.8 Mean Y = 20.0 ± 2.8 | Mean X = 23.2 ± 1.0 Mean Y = 18.8 ± 1.1 | Mean X = 21.7 ± 5.0 Mean Y = 18.9 ± 1.7 | Mean X = 24.0 ± 0.6 Mean Y = 18.9 ± 0.9 |
| Doublet Y (DY) | Mean X = 24.6 ± 1.7 Mean Y = 19.1 ± 1.8 | Mean X = 25.8 ± 0.7 Mean Y = 19.9 ± 0.6 | Mean X = 24.6 ± 0.4 Mean Y = 20.2 ± 0.2 | Not available |
| Iso | Mean X = 26.1 Mean Y = 20.3 | Mean X = 25.7 Mean Y = 20.4 | Mean X = 24.9 Mean Y = 19.1 | Mean X = 25.6 Mean Y = 18.7 |

To conclude this section, the experimental results from the first OPC iteration shows a reasonable agreement with simulation, especially on NILS where we correlate with measured dose sensitivity. To better match and improve common depth of focus, an OPC model capturing more of the lithography process effects is needed but was not part of this study. By using PSM DF mask, a 60% dose reduction can be reached however side lobe printing can be very severe with PSM DF, it is more sensitive to dose change rather than focus change. Simulation shows that PSM DF aerial image model threshold is very close to side lobe printing threshold.

4. SUMMARY

In this work, Ta and low-n masks on bright and dark mask tones are compared for logic via printing by SMO and wafer print evaluation. Simulations show that the BIM bright field Ta-based mask delivers the best RET solution for random logic via design. This agrees with line space fundamental understanding study^[9] that showed better bright field imaging. Experimental wafer results with the PSM masks do not bring much benefit on this test case. Exposure with the PSM DF suffers from side lobe printing at 6% dose variation which is within the spec limit of design target pitch X 42nm pitch y 36nm CDx 26nm CDy 18nm. In addition, the current EUV bright field mask quality on the Via target design shows larger mask CD errors than the dark field mask. Since the usage of EUV bright field mask is relatively new, mask shops need to

prioritize the bright field mask quality to enable valid experimental comparison to dark field mask imaging on wafer. PSM dark field does not seem to be the ideal candidate since printing smaller CDx to 24nm would mean that process overlay margin (x-self align) will be smaller. Different OPC strategies on PSM dark field including corner cut with smaller OPC run segment length can yield better results on random logic via designs. In future work, we would like to evaluate wafer data of this random logic via clip on both bright field and dark field Ta masks.

On the contrary, the dose reduction and NILS gain on PSM DF over BIM DF is worth to revisit using a more relax target design.

ACKNOWLEDGEMENTS

The authors are thankful to Emily Gallagher, Tatiana Kovalevich, Philippe Foubert, Paulina Rincon Delgadillo, Victor Vega Gonzalez, Sayantan Das from imec, David Rio from ASML, for their input, help and discussions.

REFERENCES

- [1] M.-Claire van Lare, Frank J. Timmermans, Jo Finders, "Alternative reticles for low-k1 EUV imaging," Proc. SPIE 11147, International Conference on Extreme Ultraviolet Lithography 2019, 111470D (26 September 2019); doi: 10.1117/12.2536415
- [2] M.-Claire van Lare et al., "Investigation into a prototype extreme ultraviolet low-n attenuated phase-shift mask" Journal of Micro/Nanopatterning, Materials, and Metrology 20(2), 021006 (21 May 2021); doi: 10.1117/1.JMM.20.2.021006
- [3] Andreas Erdmann, Peter Evanschitzky, Hazem Mesilhy, Vicky Philipsen, Eric Hendrickx, Markus Bauer, "Attenuated PSM for EUV: Can they mitigate 3D mask effects?" Proc. SPIE 10583, Extreme Ultraviolet (EUV) Lithography IX, 1058312 (19 March 2018); doi: 10.1117/12.2299648
- [4] Suhyeong Choi, Jae Uk Lee, Victor M. Blanco Carballo, Peter Debacker, Praveen Raghavan, Ryoung-Han Kim, Youngsoo Shin, Large marginal 2D self-aligned via patterning for sub-5nm technology, Proc. SPIE 10148, Design-Process-Technology Co-optimization for Manufacturability XI, 101480J (28 March 2017); doi: 10.1117/12.2257924
- [5] Suhyeong Choi, Jae Uk Lee, Victor M. Blanco Carballo, Ryoung-Han Kim, Youngsoo Shin, 2D self-aligned via patterning strategy with EUV single exposure in 3nm technology, Proc. SPIE 10143, Extreme Ultraviolet (EUV) Lithography VIII, 1014321 (24 March 2017); doi: 10.1117/12.2257923
- [6] Weimin Gao, Vincent Wiaux, Wolfgang Hoppe, Vicky Philipsen, Lawrence S. Melvin III, Eric Hendrickx, Kevin Lucas, Ryoung-han Kim, "Double patterning at NA 0.33 versus high-NA single exposure in EUV lithography: an imaging comparison," Proc. SPIE 10583, Extreme Ultraviolet (EUV) Lithography IX, 105830O (19 March 2018); doi: 10.1117/12.2297677
- [7] Anatoly Burov, Alessandro Vaglio Pret, Stewart A. Robertson, Patrick Lee, "Stochastic side-lobe printing in EUV lithography: a simulation study," Journal of Micro/Nanopatterning, Materials, and Metrology 20(3), 031009 (6 July 2021); doi: 10.1117/1.JMM.20.3.031009
- [8] Dongbo Xu, Werner Gillijns, Ling Ee Tan, Vicky Philipsen, Ryoung-han Kim, "Exploration of alternative mask for 0.33NA EUV single patterning at pitch 28nm," Proc. SPIE 11854, International Conference on Extreme Ultraviolet Lithography 2021, 118540T (12 October 2021); doi: 10.1117/12.2599054
- [9] Natalia Davydova, Jo Finders, John McNamara, Eelco van Setten, Claire van Lare, Joern-Holger Franke, Andreas Frommhold, Renzo Capelli, Grizelda Kersteen, Andreas Verch, Rene Carpaij, Joseph Zekry, Timon Fliervoet, "Fundamental understanding and experimental verification of bright versus dark field imaging," Proc. SPIE 11517, Extreme Ultraviolet Lithography 2020, 115170P (30 October 2020); doi: 10.1117/12.2573161